Structures of lithium-zinc compounds at high pressures

Structures of Lithium-Zinc Compounds at High Pressures

Philip Dalladay-Simpson,[1] Jack Binns,[1] Mengnan Wang,[1] Miriam Peña-Alvarez,[1,2] Edward J. Pace,[1,2] Eugene Gregoryanz,[1,2,3] Xiao-Jia Chen,[1] and Ross Howie[1]

[1)] *Center for High Pressure Science & Technology Advanced Research, 1690 Cailun Rd, Bldg 6, Pudong, Shanghai, 201203, P.R. China*

[2)] *Centre for Science at Extreme Conditions, The University of Edinburgh, King's Buildings, Edinburgh, UK.*

[3)] *Key Laboratory of Materials Physics, Institute of Solid State Physics, Chinese Academy of Sciences, Hefei 230031, China.*

(Dated: 17 June 2018)

Intermetallic lithium compounds have found a wide range of applications owing to their light mass and desirable electronic and mechanical properties. Here, by compressing pure lithium and zinc mixtures in a diamond-anvil cell, we observe a direct reaction forming the stoichiometric compound LiZn, at pressures below 1 GPa. On further compression above 10 GPa, we observe the formation of Li_2Zn, which is the highest lithium content compound to be discovered in the Li-Zn system. Our results constrain the structures of these compounds and their evolution with pressure, furthering our understanding of potentially useful light volume-efficient energy storage materials.

I. INTRODUCTION

The immense development of portable electronics and its market since the 1980s has warranted a vast research effort into battery design to further drive down manufacturing costs, promote their capacity and increase portability. Li-ion batteries (LIBs) are arguably the most prolific energy-storage technology currently available, finding widespread applications in automotive, telecommunication and national grid energy management.

Currently, there is interest to improve LIB performance by the generation of new higher capacity anode materials[1] resulting in lighter more powerful battery technology. Stoichiometric Li intermetallic compounds have significantly greater Li-content when compared with conventional intercalation-type carbon anodes, offering an intriguing solution to increasing LIB energy density[2]. The Li-Zn system in particular is a promising candidate, with Zn being a historically important[3] and prolific battery material primarily due to its low cost and natural abundance, exemplified by Zn-MnO_2, Zn-carbon and Zn-air being currently the most economically competitive batteries in the market.

The Li-Zn system has been extensively studied at ambient pressures; with typical synthesis techniques that involve alloying of the pure elements at high temperatures[4]. Although successful in revealing an exceedingly rich binary phase diagram, including the phases $LiZn_{13}$[5], $LiZn_4$[6], Li_2Zn_5[7], Li_2Zn_3[8] and LiZn[9], no phase exhibits a desirable molar ratio of Li to Zn greater than unity.

High pressure is an indispensable tool to further explore exotic chemistry and novel materials not observed under ambient conditions. Recent theoretical investigations on Li-rich regimes at pressure have proposed a wealth of stable stoichiometric Li_xZn intermetallic compounds with $1 < x < 4$,[10] ultimately finding the equiatomic phase LiZn to be the most energetically favourable composition up to 100 GPa. Due to the continual demand for cheaper, lighter and better performing energy storage materials, specifically for LIB batteries, it is essential to experimentally explore the synthesis of Li-rich Li-Zn compounds and to have a more complete description of lithium chemistry.

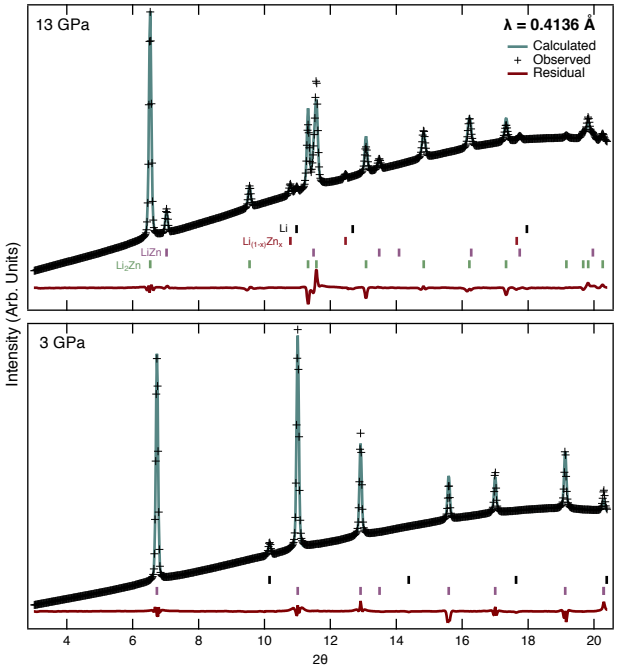

FIG. 1. Representative Rietveld refinements at 13 GPa (top panel, $wR_p = 1.13\%$, $wR_{all,Li_2Zn} = 6.86\%$, $wR_{all,LiZn} = 5.05\%$) and 3 GPa (bottom panel, $wR_p = 1.20\%$, $wR_{all,LiZn} = 10.11\%$) on compression. After synthesis of Li_2Zn on compression, trace diffraction of LiZn is observed to the highest studied pressures.

In this work, through the application of pressure, we experimentally investigated the desirable Li-rich regime of the binary Li-Zn system up to 20 GPa at room temperature. We found that at remarkably low pressures

(<1 GPa) a direct reaction between the pure elements forms the LiZn intermetallic. Upon compression above 10 GPa, Li_2Zn was synthesised, an experimentally novel intermetallic with the highest Li content in the Li-Zn system.

II. EXPERIMENTAL METHODS

High-pressure measurements were conducted in a symmetric-type diamond-anvil cell (DAC) with typical diamond culets varying from 200-300 microns in diameter. Samples were loaded in a laser-milled Re-foil gasket chamber with initial dimensions of 20-30 microns in thickness and approximately half the culet size in diameter. No pressures higher than 20 GPa were probed, due to the known pressure-enhanced diffusivity of Li into the diamond anvils leading to their premature mechanical failure[11,12]. Pressures during the experiments were determined by using the equation of state of pure Li[11], the excess reactant was detectable in all measurements, as seen in Figure 1.

High-purity Li (Alfa Aesar 99.9 %) and Zn (Alfa Aesar 99.9 %) samples were loaded under an argon-protected environment within a glove box. All samples were loaded such that the chambers in the Re-foil were first completely occupied by Li and then grains of zinc, <10 μm in diameter, were embedded. This ensured an excess of Li (estimated 1-2% Zn by volume), to encourage the exploration of the Li-rich part of the Li-Zn system, whilst also providing semi-hydrostatic conditions for synthesised samples.

Powder X-ray diffraction data were collected at the BL10XU beamline at SPring-8, Japan . The diffraction from 0.4136 Å wavelength X-rays was recorded using a digital flat-panel detector, after which it was integrated using the DIOPTAS[13] software to a two-dimensional data set. The data were subsequently indexed using GSAS-II[14]. Le Bail[15] and Rietved[16] refinement were carried out in *Jana2006*[17].

III. RESULTS AND DISCUSSION

Through the application of high pressures, we have explored the Li-rich Li-Zn system to 20 GPa at room temperature. Two intermetallics are reported, LiZn and Li_2Zn, stressing the importance of high pressure as a useful tool in exploring Li-chemistry, whereas only previous high-temperature alloying[4] or sophisticated synthesis techniques, such as molecular beam epitaxy[5], have proven successful. Analysis of the adopted high-pressure LiZn phases *via* X-ray diffraction (Figure 1), we have identified the adopted structures (Figure 2) and their pressure-evolution at room temperature (Figure 3). These results give us insight into their mechanical and electrical properties, which we compare to metrics used in choosing appropriate candidate energy-storage materials.

At remarkably low pressures, <1 GPa, we found for the first time *via* direct reaction, the formation of a LiZn intermetallic at room temperature, identified from the high-quality powder diffraction data (Figure 1 - top panel). The LiZn crystal structure was identified to be of NaTl-type (space group - $Fd\bar{3}m$) (See Figure 2 and the bottom panel in Figure 1). This structure is in agreement with well-established experimental measurements on LiZn produced by a more common metallurgical tool, high-temperature alloying, in 1933[9]. The intermetallic was stable at all pressures studied, with detectable trace diffraction detected even after the synthesis of the high-pressure Li_2Zn phase (Figure 1 - top panel), which is discussed later. The highly accessible pressure-regimes required to manipulate the alloying between these two species may be suitable for new mechanical energy harvesting analogous to piezoelectric devices[18], and has already been ingeniously applied in the Li-Si system[19]. The stability is in accordance with previous numerical calculations[10], which suggested LiZn to be the most energetically competitive phase up to 100 GPa. Calculations also indicate two possible pressure-induced structural transitions, firstly through an intermediate $Imma$ phase (45-53 GPa), before finally adopting a $Pm\bar{3}m$ structure[10]. Here, in agreement with the theory, no structural modification of the equiatomic LiZn was detected up to 20 GPa.

Upon compression above 10 GPa, we observe the formation of a novel Li_2Zn phase, appearing as a fine powder in our X-ray diffraction patterns (Figure 1 - top panel). This compound persists as the dominant phase to 20 GPa, the highest pressure reached in this study, and decomposes on decompression to LiZn at 7.4 GPa. Li_2Zn was found to adopt a hexagonal structure of AlB_2-type (space group - $P6/mmm$), seen in Figure 2, with lattice parameters $a = 4.3685$ Å and $c = 2.5509$ Å at 7.4 GPa. This structure, which is prolific in intermetallic binary and ternary systems[20], was found to have one Zn-atom occupying the 1*a* Wyckoff site (0,0,0) whilst the Li-atoms occupy the 2*d* wyckoff site $(\frac{1}{3}, \frac{2}{3}, \frac{1}{2})$. The structure is analogous to the binary lithium intermetallics produced with the Pt-group, Li_2M (where M = Pd, Pt)[21,22], with lithium forming graphene-like planes with the transition metal atoms contained between (see Figure 2). Although the first experimental report of Li_2Zn, this phase has been seen previously in recent numerical calculations[10], which further reported a structural change to another orthorhombic phase (also space group symmetry $Imma$) above 80 GPa, which was out of the scope of this study. Recent calculations have reported the thermodynamic stability of Li:Zn with stoichiometry 1:1 and 2:1[10], albeit finding the 1:1 ratio to be the most stable up to 100 GPa. Here, Li_2Zn was observed and found to be the dominant phase above pressures of 7.4 GPa (see Figure 1 - top panel). We therefore find that the relative abundance of the coexisting phases are primarily driven by

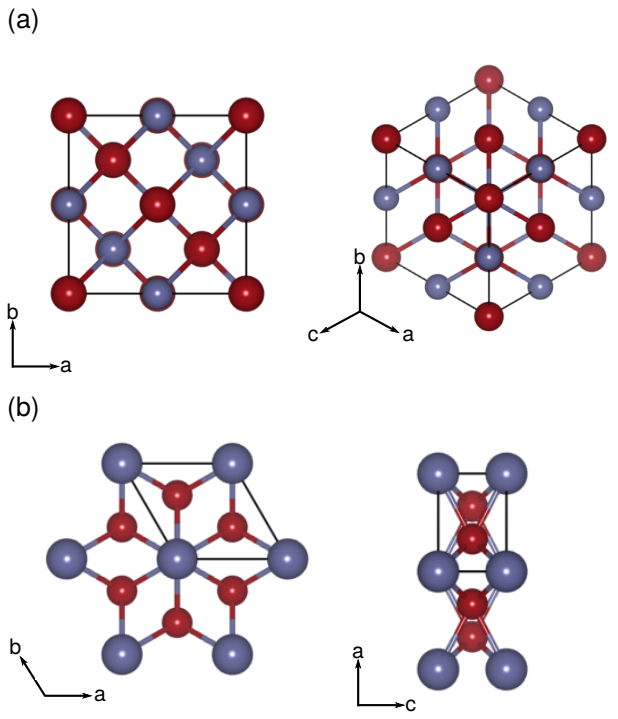

FIG. 2. Crystal structures observed in the Li-Zn system at high pressures, Li atoms are red whilst Zn atoms are blue.(a) The equiatomic LiZn intermetallic, a NaTl-type structure ($Fd\bar{3}m$) with interlocking Li and Zn diamond sublattices. (b) Li_2Zn ($P6/mmm$) formed on compression above 10 GPa, where Zn atoms are encapsulated in a hexagonal prism comprised of 12 Li atoms.

the initial concentration of the constituent elements.

As mentioned previously, in both the high-pressure intermetallic compounds, LiZn and Li_2Zn, the Li atoms are constrained by symmetry to special positions within their respective structures. Therefore, despite the weak scattering of lithium, it is still possible to extract Li-Zn bond distances which are summarised in Figure 4. It is found that in LiZn, the Zn is encapsulated by a total of 10 Li atoms; 4 nearest neighbours and 6 next-nearest neighbours (NNNs are represented in Figure 4(a) as the face-centred Li atoms), measured to be 2.470(2) Å and 2.852(2) Å respectively at 19.3 GPa. Whilst the Zn atoms in Li_2Zn are found to lie within hexagonal cages consisting of 12 equally spaced Li atoms varying from distances of 2.825(4) Å to 2.633(3) Å in the pressure range covered, 7.4 to 19.3 GPa.

Interestingly, Li_2Zn is found to have comparable Zn-Li distances to the average distances reported in the LiZn compound, despite being the higher pressure phase, seen in figure 4(b). In fact, the values are found to exactly match at the Li_2Zn formation pressure, 2.825(4) Å at 7.4 GPa. The similarity of these values is a demonstration of the pressure-distance paradox[23], *i.e.* an increase in co-ordination of the Zn atoms, rather than a continual reduction in Zn-Li seperation over the pressure regime studied.

Additionally to the previously mentioned stoichiometric phases, a non-stoichiometric Zn-alloyed lithium phase ($Li_{1-x}Zn_x$) was also observed (see Figure 1-top panel and figure 3(c)). The signature of the alloying can be readily seen above 10 GPa, where Bragg peaks of Li were shadowed by an identical set of reflections shifted to slightly lower 2θ, seen in Figure 1-top panel. These diffraction rings could only be observed in regions containing LiZn/Li_2Zn and were not observed in the surrounding excess Li. The marginal volume expansion of the Li is attributed to Zn partially dissolved in Li (see figure 3(c)), slightly expanding the Li lattice. The percentage of alloying was estimated *via* a volume analysis of the pure species[11][24], where no interspecies charge transfer is assumed. It is found to be at a maximum of 6% at 9.9 GPa (shown in Figure 3(c)), diminishing almost linearly with pressure to 2%. The expulsion/inclusion of Zn in the host Li accounts for the seemingly large compressibility of this alloy when compared with pure Li, seen in Figure 3(c). The solubility of Zn was observed to be independent on the pressure path as seen by being reversible on decompression. The effect of Zn-alloying on the rich phase diagram Li could have implications for its low-temperature superconductivity[25], cold melting[12] and exotic higher pressure phases[12].

Complete understanding of the mechanical properties of materials are a key a metric in battery design. This is especially the case for LIBs, whereby the process of (de)lithiation can result in significant volume changes[2], for example $Li_{15}Si_4$ reports a 280% expansion[26], which therefore need to be accomodated in the battery architecture. We find that Zn has a typical expansion of 98% at 0.7 GPa when forming the LiZn intermetallic, in good agreement with previous results[2,9] and roughly a tenfold increase when compared with conventional intercalation-graphite anodes used in current LIBs[2]. The relative expansion is found to be weakly pressure independent falling by 13% over the entire pressure regime studied. Consequently, Li_2Zn shows a significant 205% volume increase at 7.4 GPa when compared to unlithiated Zn, unsurpisingly, it is approximately a two-fold increase when compared with the volume expansion of the equiatomic LiZn phase for the same pressure.

The bulk and linear moduli of LiZn and Li_2Zn as a function of pressure were calculated, using procedures in EoSfit7[27], and are summarised by Table I. The fitted lattice parameters of the unit cells and their respective volumes were found to be well described by the 3^{rd} order Birch-Murnaghan relation[28]. The Li_2Zn structure was found to exhibit moderate anisotropic compressibility, with a two-fold greater linear compressibility along the *a*,*b*-axis when compared to the *c*-axis, see table I. Intuitively, this can be seen as the hexagonal planes of Li being more susceptible to compression, opposed to the linear chains of Zn atoms which lie in parallel to the *c*-

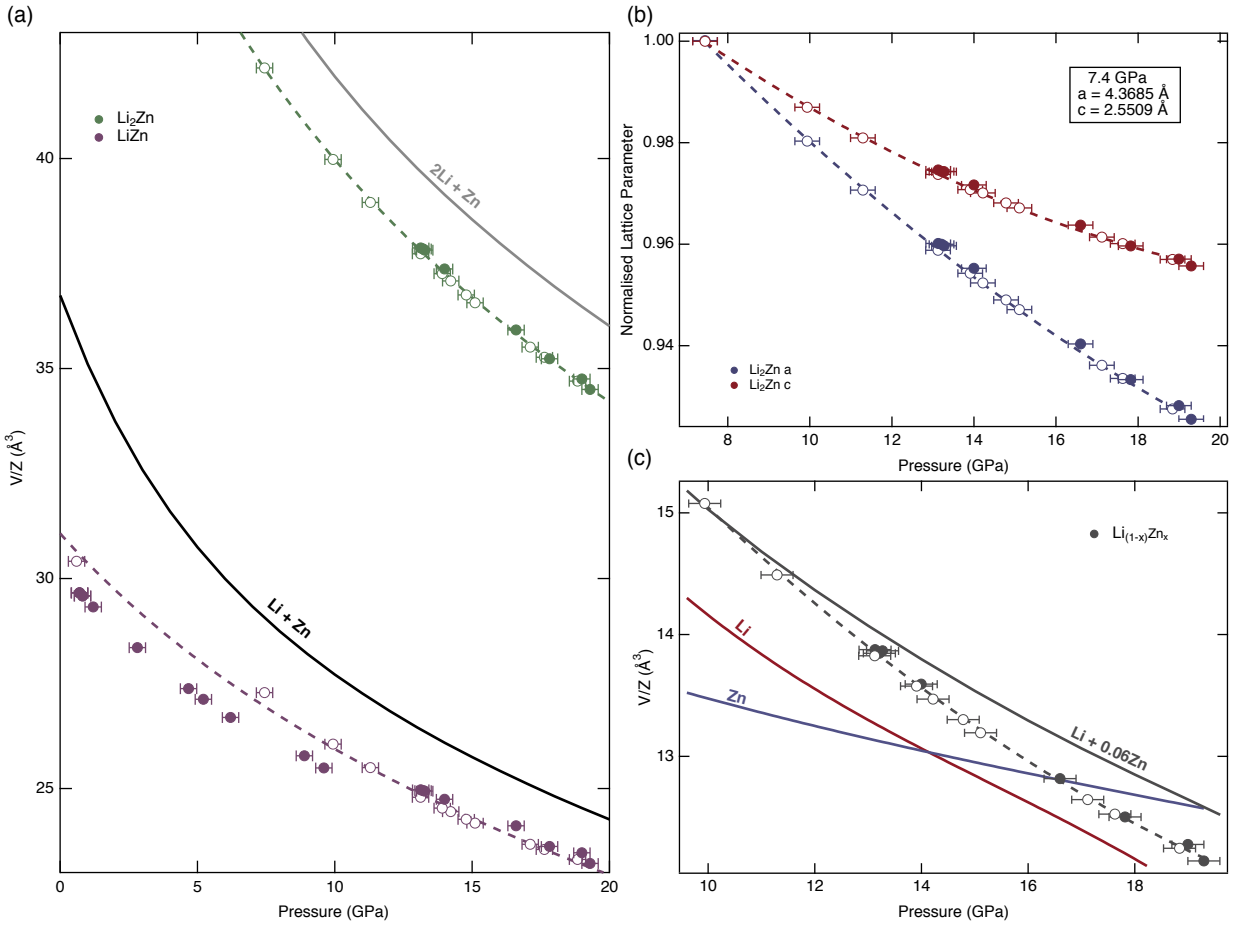

FIG. 3. **(a)** Volume per formula unit curves of LiZn (purple circles) and Li_2Zn (green circles), plotted alongside known volume curves of Li+Zn (black line) and 2Li+Zn (grey line).**(b)** The normalised lattice parameters a (blue circles) and c (red circles) of the Li_2Zn structure with pressure.**(c)** Volume per formula unit curves of the non-stoichiometric alloy ($Li_{1-x}Zn_x$), observed as volume-expanded *fcc*-Li peaks in the integrated patterns (figure 1-top panel), alongside Li (red), Zn (blue) and Li+0.06Zn (grey). In all figures data on compression and decompression are shown as filled and empty symbols respectively.

TABLE I. Refined parameters of 3^{rd} order Birch-Murnaghan equation-of-state fits for LiZn and Li_2Zn, plotted in Figure 3. The zero-pressure structural parameters of LiZn and Li_2Zn are given: volume - V_0, lattice constants - a_0 and c_0. The bulk (B_0) and linear modulii (M_0) with their respective pressure derivatives at zero-pressure, B' and M', are also included.

	Space Group	**V_0 (Å^3)**	**Lattice Parameter (Å)**	**B_0 (GPa)**	**B'**	**M_0 (GPa)**	**M'**
LiZn	$Fd\bar{3}m$	249(7)	$a_0 = 6.29(2)$	42(13)	3.1(11)	127(14)	9.3(12)
Li_2Zn	$P6/mmm$	53(3)	$a_0 = 4.75(8)$	22(8)	3.5(6)	61(19)	9.3(11)
			$c_0 = 2.7623(6)$			32(3)	30(4)

axis, seen in Figure 2 and quantified in Figure 3b. The measured volume of Li_2Zn was found to be completely reversible on decompression, although found to be stable to lower pressures than when originally synthesised, 7.4 GPa, seen in Figure 1. In contrast however, a small but notable deviation unit cell volume and pressure path for LiZn was observed. An effect which can be readily seen in the experimental data provided, see Figure 3 A, with the unit cell of LiZn found to be 0.8 Å^3 smaller on compression up to 10 GPa with respect to values measured on decompression. The deviation is attributed to the sample not in a fully equilibriated state, whereby insufficient time has been given during the course of the compression for the complete lithiation of Zn, consequently resulting in a reduced unit-cell volume. In both intermetallics, LiZn and Li_2Zn, the evolution of the unit cell volume

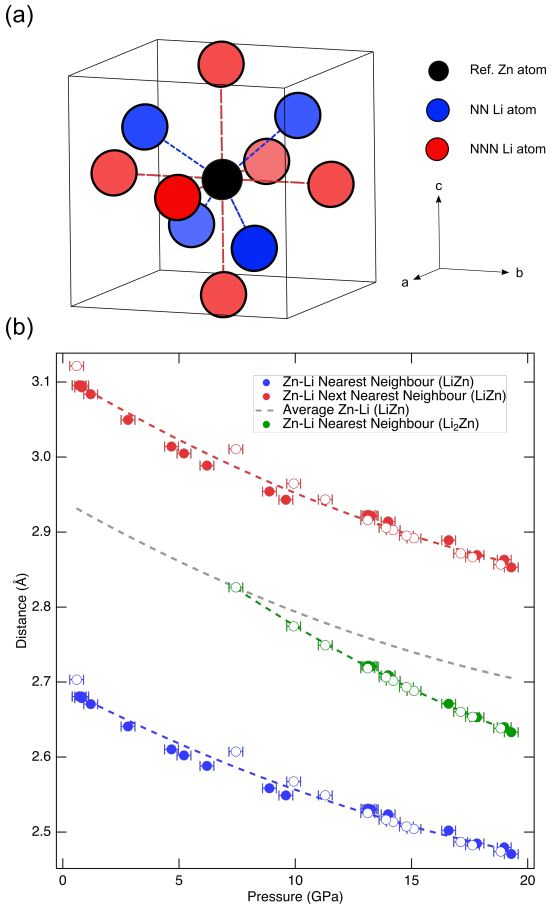

FIG. 4. **(a)** Structural model of the unit cell of LiZn omitting all atoms apart from a reference Zn atom and its nearest and next nearest neighbouring Li atoms, coloured black, blue, and red respectively. **(b)** Distances between Zn and its neighbouring Li atoms in their respective structures: LiZn - nearest (blue) and next nearest (red), Li_2Zn - nearest (green). The grey dashed line represents the average Zn-Li distance of the LiZn intermetallic. Data on compression and decompression are shown as filled and empty symbols respectively

corresponds well with that of the relative equations of state for the formula units of the pure species (Li+Zn for LiZn and 2Li+Zn for Li_2Zn), seen in Figure 3 A, further establishing the correct stoichiometry. Small reductions in volumes were found, for example at 14 GPa 1.3 Å^3 for LiZn and 1.7 Å^3 for Li_2Zn relative to the EoS of the pure species formula units, indicative of charge transfer inherent to intermetallic compounds and in agreement with previous Bader charge analysis of Li-Zn compounds[10].

Finally, theoretical capacities (Q_T) were calculated using Faraday's law of electrolysis, where: n_{Li} is the number of Li-ions involved in the (de)lithitaion process, F is Faraday's constant and M_w is the molar weight.

$$Q_T[mAhg^{-1}] = \frac{n_{Li}F}{36M_w} \quad (1)$$

Therefore, assuming complete charge/discharge of zinc can be exploited, the realization of the Li_2Zn means that a potential capacity of 676 mAhg^{-1} is available in the Li-Zn system. Found to be greater than a twofold increase, when compared with conventionally used carbon anodes, 372 mAhg^{-1}[29]. Intriguingly, this result could also explain anomalously large discharges reported in previous Zn-anode Li-ion battery studies[30], suggesting that although Li_2Zn is not found to be quenchable to ambient pressures, there might be possibility to stabilise it electrochemomechanically.

IV. CONCLUSIONS

In summary, using high-pressure powder X-ray diffraction, we have explored the Li-rich Li-Zn system up to 20 GPa at room temperature. We have verified the synthesis of both LiZn and Li_2Zn upon compression, the latter possessing the highest Li-molar content in the respective binary system. We report that the synthesised LiZn intermetallic to be the previously well-established NaTl-type structure[9] and was present at all pressures studied. Additionally, Li_2Zn was synthesised on compression above 10 GPa, adopting a hexagonal structure in agreement with recent theoretical calculations[10], as well as analogous to other previously reported binary Li-intermetallics[21]. These results are important in the quest for new higher capacity Li-bearing materials and could find applicability in future battery design.

ACKNOWLEDGMENTS

PD-S and RTH acknowledge their respective "1000 talents" awards and that of H-K Mao. MP-A acknowledges the support of the European Research Council (ERC) Grant Hecate reference No. 695527. Parts of this research were conducted at the SPring-8 facility under proposal No. 2017A1401, we would like to thank Naohisa Hirao and Saori Imada-Kawaguchi for their assistance during the course of the data collection.

[1] N. Nitta and G. Yushin, Particle and Particle Systems Characterization **31**, 317 (2014).
[2] M. N. Obrovac and V. L. Chevrier, Chemical Reviews **114**, 11444 (2014).
[3] A. Volta, Philosophical Transactions of the Royal Society of London **90**, 403 (1800).
[4] A. D. Pelton, Journal of Phase Equilibria **12**, 42 (1991).
[5] D. Fischer and M. Jansen, Zeitschrift für anorganische und allgemeine Chemie **636**, 1917 (2010).
[6] H. Schonemann and H.-U. Schuster, Rev. Chim. Min. **13**, 32 (1976).
[7] E. Zintl and A. Schneider, Zeitschrift für Elektrochemie **41**, 764 (1935).
[8] A. Baroni, IX Congr. Int. Quim. Pura Appl. **2**, 464 (1935).
[9] E. Zintl and G. Brauer, Zeitschrift für Physikalische Chemie B **20**, 245 (1933).
[10] H. Bi, S. Zhang, S. Wei, J. Wang, D. Zhou, Q. Li, and Y. Ma, Physical Chemistry Chemical Physics **18**, 4437 (2016).
[11] M. Hanfland, I. Loa, K. Syassen, U. Schwarz, and K. Takemura, Solid State Communications **112**, 123 (1999).

[12]C. L. Guillaume, E. Gregoryanz, O. Degtyareva, M. I. McMahon, M. Hanfland, S. Evans, M. Guthrie, S. V. Sinogeikin, and H.-K. Mao, Nature Physics **7**, 211 (2011).
[13]C. Prescher and V. B. Prakapenka, High Pressure Research **35**, 223 (2015).
[14]B. H. Toby and R. B. Von Dreele, Journal of Applied Crystallography **46**, 544 (2013).
[15]A. Le Bail, H. Duroy, and J. Fourquet, Mater. Res. Bull. **23**, 447 (1988).
[16]H. M. Rietveld, J. Appl. Crystallogr. **2**, 65 (1969).
[17]V. Petříček, M. Dušek, and L. Palatinus, Z. Krist. - Cryst. Mater. **229**, 345 (2014).
[18]J. Granstrom, J. Feenstra, and H. Sodano, Smart Materials and Structures **16** (2007).
[19]S. Kim, S. J. Choi, K. Zhao, H. Yang, G. Gobbi, S. Zhang, and J. Li, Nature Communications **7**, 10146 (2016).
[20]P. Villars and L. D. Calvert, *Person's Handbook of Crystallographic Data for Intermetallic Phases*, 2nd ed. (American Society for Metals, American Society for Metals, Materials Parkm OH 44073, 1991).
[21]W. Bronger, B. Nacken, and K. Ploog, Journal of the Less Common Metals **43**, 143 (1975).
[22]J. H. N. van Vucht and K. H. J. Buschow, Journal of the Less Common Metals **48**, 345 (1976).
[23]W. Kleber and K. T. Wilke, Kristall und Technik , 165 (1969).
[24]T. Kenichi, Physical Review B **56** (1997).
[25]T. H. Lin and K. J. Dunn, Physical Review B **33**, 807 (1986).
[26]M. Zeilinger, V. Baran, L. van Wüllen, U. Häussermann, and T. F. Fässler, Chemistry of Materials **25**, 4113 (2013).
[27]J. Gonzalez-Platas, M. Alvaro, F. Nestola, and R. J. Angel, Journal of Applied Crystallography **49**, 1377 (2016).
[28]F. Birch, Physical Review **71**, 809 (1947).
[29]S. Yata, H. Kinoshita, M. Komori, N. Ando, A. Anekawa, and T. Hashimoto, in *Extended Abstracts of 60th Annual Meeting of the Electrochemical Society of Japan* (1993).
[30]Y. Hwa, J. H. Sung, B. Wang, C.-M. Park, and H.-J. Sohn, Journal of Materials Chemistry **22**, 12767 (2012).